The Journal of Neuroscience, May 15, 1996, 16(10):3322–3333

A Novel Entorhinal Projection to the Rat Dentate Gyrus: Direct Innervation of Proximal Dendrites and Cell Bodies of Granule Cells and GABAergic Neurons

Thomas Deller,[1] Albert Martinez,[2] Robert Nitsch,[3] and Michael Frotscher[1]

[1]Institute of Anatomy, University of Freiburg, D-79001 Freiburg, Germany, [2]Departamento de Biologia Cellular Animal i Vegetal, Universitat de Barcelona, 08028 Barcelona, Spain, and [3]Institute of Anatomy, Humboldt University Clinic (Charité), 10098 Berlin, Germany

Entorhinal fibers to the fascia dentata originating from layer II stellate neurons are known to terminate exclusively in the outer two thirds of the molecular layer, where they innervate distal dendritic portions of dentate neurons. Using anterograde tracing with *Phaseolus vulgaris* leucoagglutinin, we unraveled a previously unknown entorhinal projection that directly innervates proximal dendritic portions and somata of granule cells and GABAergic neurons. This projection originates from neurons located in entorhinal layers IV–VI of the medial entorhinal area. These fibers enter the outer two thirds of the molecular layer, traverse the inner molecular layer (IML) and granule cell layer, where they form numerous boutons, and finally arborize subjacent to the granule cells. Correlated light and electron microscopy revealed that the boutons formed by these fibers establish asymmetric synapses on dendrites in the IML, on spines and somata of granule cells, and on spineless dendrites subjacent to the granule cell layer. Postembedding immunogold staining indicates that this entorhino-dentate projection is not GABAergic and that it also terminates on GABAergic inhibitory neurons. These data demonstrate that not all entorhino-dentate fibers display a similar high laminar specificity for the outer molecular layer (OML). Although fibers from the superficial layers of the entorhinal cortex terminate exclusively in the OML, entorhinal fibers arising from deeper layers are not confined to laminar boundaries. Finally, the possibility that these supposedly excitatory entorhinal afferents may monosynaptically activate proximal dendrites and somata of dentate neurons needs to be incorporated into contemporary concepts of the hippocampal network.

Key words: entorhino-hippocampal interaction; perforant pathway; feedforward inhibition; GABA-postembedding; laminar specificity; Phaseolus vulgaris *leucoagglutinin*

Entorhinal fibers make up the major extrinsic input to the rat dentate gyrus. These fibers are believed to terminate exclusively in the outer two thirds of the dentate molecular layer, where they form synapses on dendrites of granule cells and local circuit neurons (for review, see Amaral and Witter, 1995). Because of this strict lamination, the outer part of the dentate molecular layer often is referred to as the "entorhinal zone," whereas the inner one third, where associational and commissural fibers from the polymorph layer of the dentate gyrus terminate (Blackstad, 1956; Zimmer, 1971; Swanson et al., 1978, 1981; Deller et al., 1994, 1995), is called the "hippocampal zone." Contrary to this model of strict lamination of dentate afferents, degenerated entorhinal terminals were reported in the inner molecular layer (IML) of the dentate gyrus after entorhinal lesion (Lee et al., 1977), suggesting the existence of a yet unknown entorhinal projection to the IML. Evidence for such an entorhinal projection to the "hippocampal zone" of the dentate gyrus would call for a reconsideration and modification of the present concept of lamination in the dentate gyrus in which it generally is assumed that the hippocampal zone of the dentate gyrus is entirely devoid of entorhinal fibers. Moreover, a direct entorhinal innervation of proximal dendritic portions and somata of dentate neurons would need to be incorporated into our current understanding of the physiology of the entorhino-hippocampal interaction.

In the present study, we have used the anterograde tracer *Phaseolus vulgaris* leucoagglutinin (PHAL), which labels the course of individual axons (Gerfen and Sawchenko, 1984; Deller et al., 1995) and allows for a description of the trajectory and termination pattern of fibers. PHAL tracing of entorhinal fibers revealed a novel entorhinal projection that terminates outside the "entorhinal zone" of the dentate gyrus. Postembedding immunocytochemistry for GABA was used to determine the transmitter phenotype of these anterogradely labeled entorhinal fibers and their targets.

MATERIALS AND METHODS

Sixteen male and female Sprague–Dawley rats (250–350 gm) housed under standard laboratory conditions were used in this study. Surgical procedures were performed under deep anesthesia (Nembutal, 50 mg/kg body weight). PHAL [2.5% in 10 mM phosphate buffer (PB), pH 7.8 (Vector Laboratories, Burlingame, CA)] was delivered iontophoretically (Gerfen and Sawchenko, 1984) into the entorhinal cortex using a glass micropipette (tip diameter, 15–30 μm, 5 μA positive current, on-period/off-period 5 sec for 20–30 min). Ten animals received PHAL injections into the medial entorhinal cortex (coordinates from bregma: anteroposterior, −8.5; lateral, 3.8–4.5; ventral, 5.8) (Paxinos and Watson, 1986), another six animals received PHAL injections into the lateral entorhinal cortex (coordinates from bregma: anteroposterior, 8.6; lateral, 5.0–6.0; ventral, 5.8) (Paxinos and Watson, 1986). Four animals with PHAL injections into the medial entorhinal area were used for postembedding immunogold staining for GABA. The animals were allowed to survive for 10 d after the injection of the anterograde tracer. Afterward, the rats were

Received Nov. 2, 1995; revised Feb. 12, 1996; accepted Feb. 19, 1996.

This work was supported by the Deutsche Forschungsgemeinschaft (Fr 620/4-2; Ni 344/1-1; Ni 344/5-1; and Leibniz Program), and CIRIT BE94/Annex 1–4 to A.M. We thank A. Schneider, R. Kovacs, and M. Winter for excellent technical assistance.

Correspondence should be addressed to Dr. Thomas Deller, Anatomisches Institut I, Postfach 111, 79001 Freiburg, Germany.

anesthetized deeply with Nembutal and perfused transcardially with a fixative containing 4% paraformaldehyde, 0.1% glutaraldehyde, and 15% picric acid in 0.1 M PB, pH 7.4. Animals used for postembedding immunostaining for GABA were perfused with a fixative containing 2.5% paraformaldehyde, 1% glutaraldehyde, and 0.2% picric acid in 0.1 M PB. Brains were removed and post-fixed for 2 hr in glutaraldehyde-free fixative; 100-μm-thick sections (cut in the horizontal or frontal plane) were sectioned on a vibratome and washed in PB.

Immunocytochemistry was used to visualize PHAL-containing axons. Free-floating sections were incubated for 2 d at 4°C in biotinylated goat anti-PHAL (1:400) (Vector Laboratories), 1% normal horse serum, and 0.1% NaN_3 in 0.1 M PB. For light microscopy, the antibody solution also contained 0.5% Triton X-100. After rinsing in PB, the sections were incubated in the intensified avidin–biotin–peroxidase complex (ABC-Elite, Vector Laboratories) for 3 hr. After three subsequent washes, the sections were immersed in a nickel–diaminobenzidine (DAB) solution (0.05% 3,3′ DAB, 0.02% nickel ammonium chloride, 0.024% cobalt chloride, 0.001% H_2O_2, in 0.1 M PB, for 5–10 min), which resulted in a deep-blue labeling of PHAL-containing fibers. Animals used for postembedding iummunostaining for GABA were reacted with DAB alone (0.05% 3,3′ DAB, 0.001% H_2O_2, in 0.1 M PB, for 5–10 min). Sections for light microscopy were placed on gelatin-coated slides, dehydrated in ethanol, and mounted in hypermount (Life Science International, Frankfurt, Germany). The sections for electron microscopy were osmicated (0.5% OsO_4 in PB, for 30 min), dehydrated (70% ethanol containing 1% uranyl acetate), and embedded in Durcopan (ACM) between liquid release–coated slides and coverslips. Selected sections were reembedded in blocks, and ultrathin sections collected on single-slot Formvar-coated copper grids were contrasted with lead citrate and examined in a Zeiss electron microscope. Sections processed for postembedding immunostaining for GABA were reembedded for ultrathin sectioning, and serial thin sections were cut and mounted on nickel grids.

The immunogold staining procedure followed that described by Somogyi and Hodgson (1985), using a commercially available antiserum against GABA (Sigma, St. Louis, MO). The immunostaining was carried out on droplets of Millipore-filtered solutions in humid Petri dishes. Briefly, immersion in 1% periodic acid (10 min) was followed by washing in several changes of double-distilled water. Thereafter, the grids were transferred through 2% sodium metaperiodate (10 min) and washed in several changes of double-distilled water and three changes of Tris-buffered saline (TBS), pH 7.4. After preincubation in 1% ovalbumin dissolved in TBS (30 min), the grids were incubated overnight in a rabbit anti-GABA antiserum (Sigma) (1:5000, in 1% normal goat serum in TBS). After rinsing in TBS and 50 mM Tris buffer, pH 7.4, containing 1% bovine serum albumin and 0.5% Tween 20 (10 min), the grids were incubated in the secondary antibody (goat anti-rabbit IgG-coated colloidal gold, 15 nm) for 2 hr (diluted 1:10, in darkness). After rinsing in 2% glutaraldehyde (10 min) the grids again were washed in double-distilled water and stained with uranyl acetate and lead citrate. In control experiments, the primary GABA antibody was omitted. No immunogold labeling occurred under these conditions.

RESULTS

Injection sites

All animals received a single PHAL deposit into the entorhinal cortex (Fig. 1*a*). The injection sites were found in the medial and lateral entorhinal areas and usually covered several cell layers (Fig. 1*b*). Injection sites varied in diameter between 100 and 800 μm. An increased immunocytochemical background staining could be observed for an additional 100–500 μm beyond the central injection site. In this peripheral zone of the injection site, no PHAL-labeled cells could be observed. The cell-poor lamina dissecans (layer IV) often separated superficial PHAL-injection sites (layers I–III) from deeper entorhinal cell layers, which made it possible to correlate injection sites with the cell layers of the entorhinal cortex (Fig. 1*a*,*b*). The dorso-ventral extent of the injection sites also was reconstructed using consecutive horizontal sections of the entorhinal cortex. Injection sites varied between 500 and 800 μm in their longitudinal extent.

The "classical" entorhinal projection terminates in the outer molecular layer (OML)

As shown in detail earlier (Steward, 1976; Wyss, 1981; Deller et al., 1996) (for review, see Amaral and Witter, 1995), the entorhino-dentate projection from layer II of the entorhinal cortex terminates exclusively in the outer two thirds of the molecular layer. This "classical" entorhino-dentate projection was labeled heavily after PHAL injections into the entorhinal cortex. Tracer deposits located in the medial entorhinal area labeled the entorhino-dentate projection to the middle one third of the OML, whereas tracer deposits located in the lateral entorhinal area labeled the entorhino-dentate projection to the outer one third of the molecular layer. In agreement with earlier reports, this entorhino-dentate projection showed the topography typical of the perforant pathway (Steward, 1976; Wyss, 1981) (for review, see Amaral and Witter, 1995) (Fig. 9).

A novel entorhinal projection terminates in the IML, granule cell layer, and hilus

We were struck by another group of entorhino-dentate fibers that left the OML of the dentate gyrus and entered the inner molecular zone, perforated the granule cell layer, and eventually collateralized subjacent to the granule cell layer (Fig. 2). This projection was present in male and female rats. These fibers entered the fascia dentata via the crest of the dentate gyrus and collateralized in the outer two thirds of the molecular layer (Fig. 2*a–c*), where they formed numerous boutons and short axonal extensions. Within the OML, these fibers branched off axon collaterals to the IML, granule cell layer, and hilus. These collaterals left the outer two thirds of the molecular layer at oblique and perpendicular angles and entered the inner one third of the molecular layer (Fig. 2*c*). There, these entorhinal fibers heading to the hilus rarely branched, but formed numerous boutons and a large number of short axonal extensions (Fig. 2*d*, *e*). These axons traversed the granule cell layer, where some collaterals formed pericellular baskets on cell bodies (Figs. 2*c*, 5*a*). After entering the hilus, the entorhinal fibers continued subjacent to the granule cells, where they formed numerous varicosities (Figs. 2*c*, 6*a*). Only rarely did we observe axonal extensions arising from these fibers in the granule cell layer and hilus. Only occasionally, thin collaterals entered the deep hilar region (Fig. 2*c*), where they formed multiple en passant boutons (Figs. 2*c*, 6*d*). A small number of these axons traversed the entire hilus and terminated subjacent to the granule cells of the opposite blade of the dentate gyrus.

Proximal dendrites and somata of granule cells and GABAergic neurons are targets of entorhinal fibers

Correlated light and electron microscopy of PHAL-labeled entorhinal fibers in the IML revealed asymmetric synapses with the shafts of dendrites (Fig. 3*a–d*). All synapses of these entorhinal axons found in the IML were asymmetric (Fig. 3*b–d*). Postembedding immunocytochemistry for GABA was used to characterize further some of the target structures of entorhinal axons in the IML. The postembedding immunocytochemistry was highly specific, and only very low levels of unspecific background labeling were observed (Fig. 4*a*). Serial sections of PHAL-labeled terminals were examined, and some of these terminals established synapses that appeared to be asymmetric on dendrites of GABAergic neurons (Fig. 4*d–f*).

Within the granule cell layer, we observed exclusively asymmetric synapses on dendrites (Fig. 4*a–c*), the somata (Fig. 5*b*), and

Figure 1. PHAL injection sites. *a*, Horizontal section of the entorhinal cortex showing a PHAL injection site in the deep layers of the medial entorhinal area. The center of the injection site is indicated with an *arrow* in *b*. The dentate gyrus of the same animal is illustrated in Figure 2. *b*, Schematic drawing of PHAL injection sites. *Open circles* indicate the central areas (200–300 μm in diameter) of the injection sites. The injection site of the animal shown in *a* is indicated with an *arrow*. Scale bars: *a*, 500 μm; *b*, 750 μm.

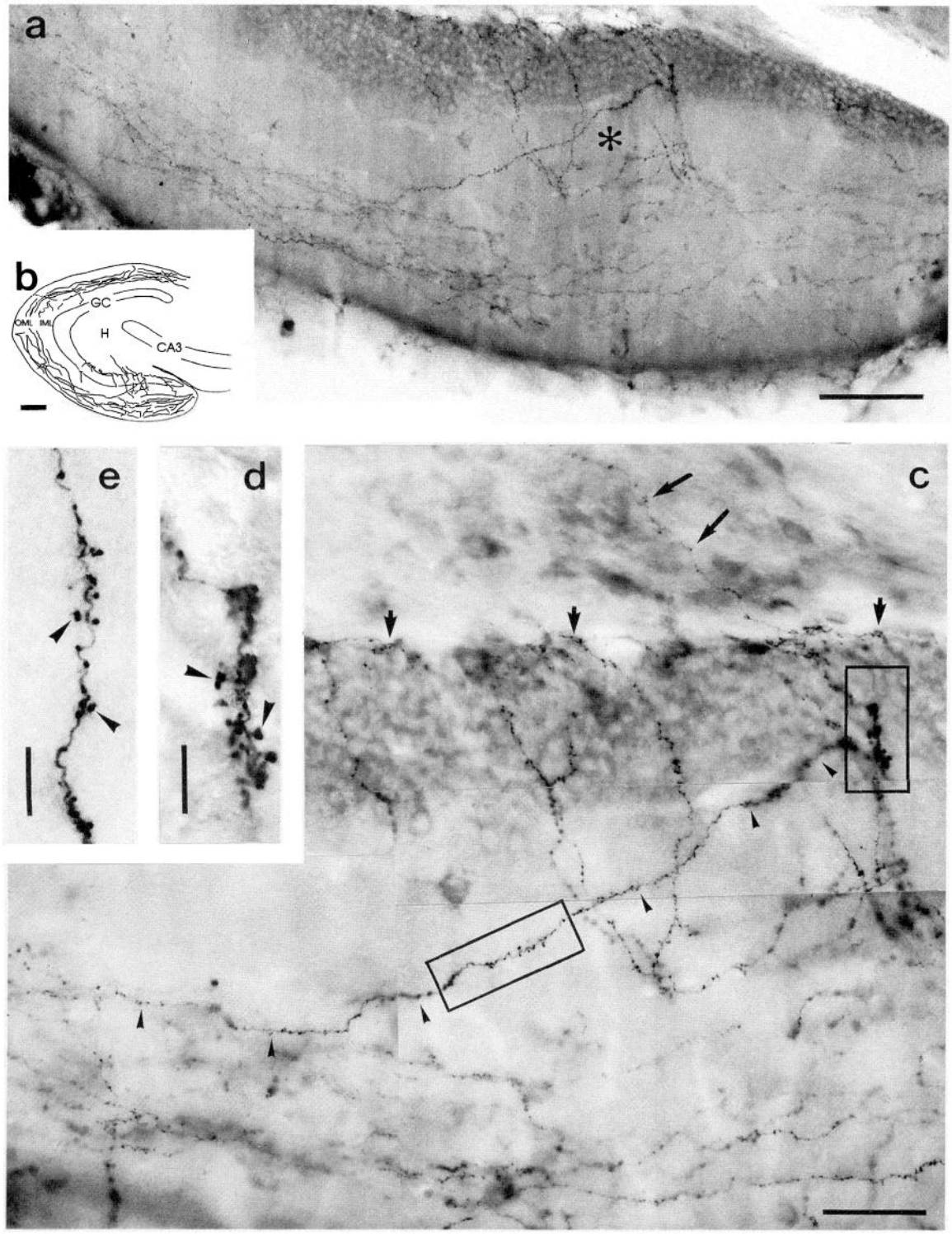

Figure 2. Entorhinal fibers to the IML, granule cell layer, and hilus. *a*, Infrapyramidal blade of the dentate gyrus shown in *b*. The injection site of this animal is shown in Figure 1*a*. PHAL-labeled entorhinal fibers are found in the outer two-thirds of the molecular layer, where they run in parallel to the granule cell layer. Some entorhinal fibers leave the outer molecular zone and reach the hilar area via the IML and granule cell layer. Area indicated with an *asterisk* is shown at higher magnification in *c*. *b*, Camera lucida drawing of the dentate gyrus of the case illustrated in Figure 1*a*. PHAL-labeled entorhinal fibers to the IML, granule cell layer, and hilus are located preferentially in the infrapyramidal blade of the dentate gyrus, which is illustrated at higher magnification in *a* and *c*. *c*, Higher magnification of the area indicated with an *asterisk* in *a*. PHAL-labeled entorhinal fibers form numerous boutons in the OML, IML, granule cell layer, and hilus. One fiber can be followed from the OML to the granule cell layer (*arrowheads*). Within the IML and granule cell layer, these fibers form numerous axonal extensions. Framed area on the *left* is shown at higher magnification in *e*, framed area on the *right* is shown at higher magnification in *d*. These entorhinal fibers continue to the hilus, where the majority terminates subjacent to the granule cell layer (*short bold arrows*). A few axons continue into the hilar area (*long bold arrows*). *d*, Higher magnification of framed area (*right*) in *c*. Note axonal extensions leaving the main axon in the granular layer (*arrowheads*). *e*, Higher magnification of framed area (*left*) in *c*. Axonal extensions leave the main axon in the IML (*arrowheads*). Scale bars: *a*, 80 μm; *b*, 125 μm; *c*, 40 μm; *d*, *e*, 10 μm.

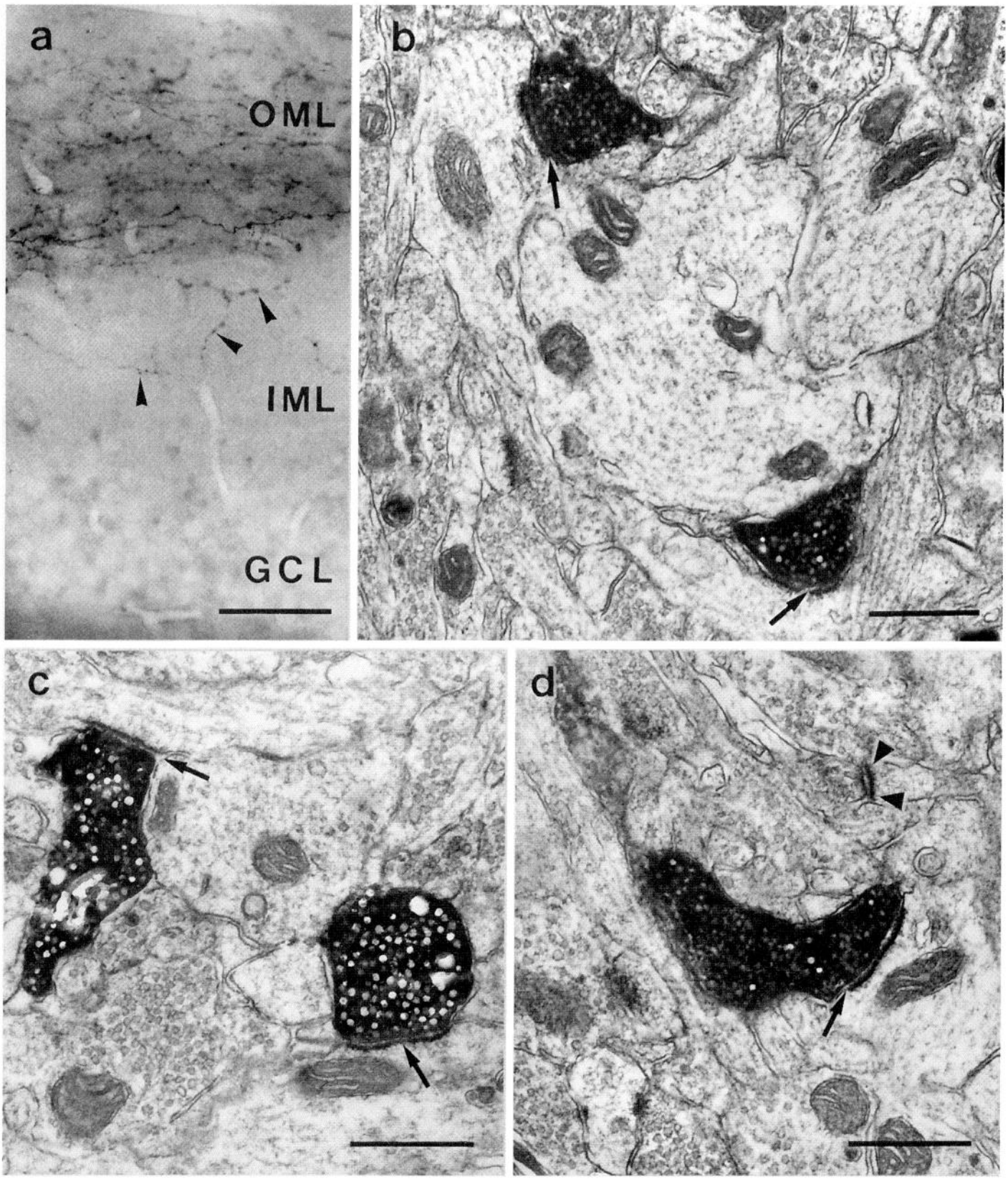

Figure 3. Correlated light and electron microscopy of PHAL-labeled entorhinal fibers in the IML of the dentate gyrus. *a*, Light micrograph of a section embedded for electron microscopy. *Arrowheads* indicate PHAL-labeled entorhinal fibers in the IML. Electron micrographs of this section shown in *b–d*. *b–d*, PHAL-labeled entorhinal terminals forming asymmetric synapses with dendritic shafts in the IML. *Arrows* point to the synaptic clefts. *Arrowheads* in *d* label an unstained terminal forming an asymmetric synapse with a neighboring spine. Scale bars: *a*, 40 μm; *b–d*, 0.5 μm.

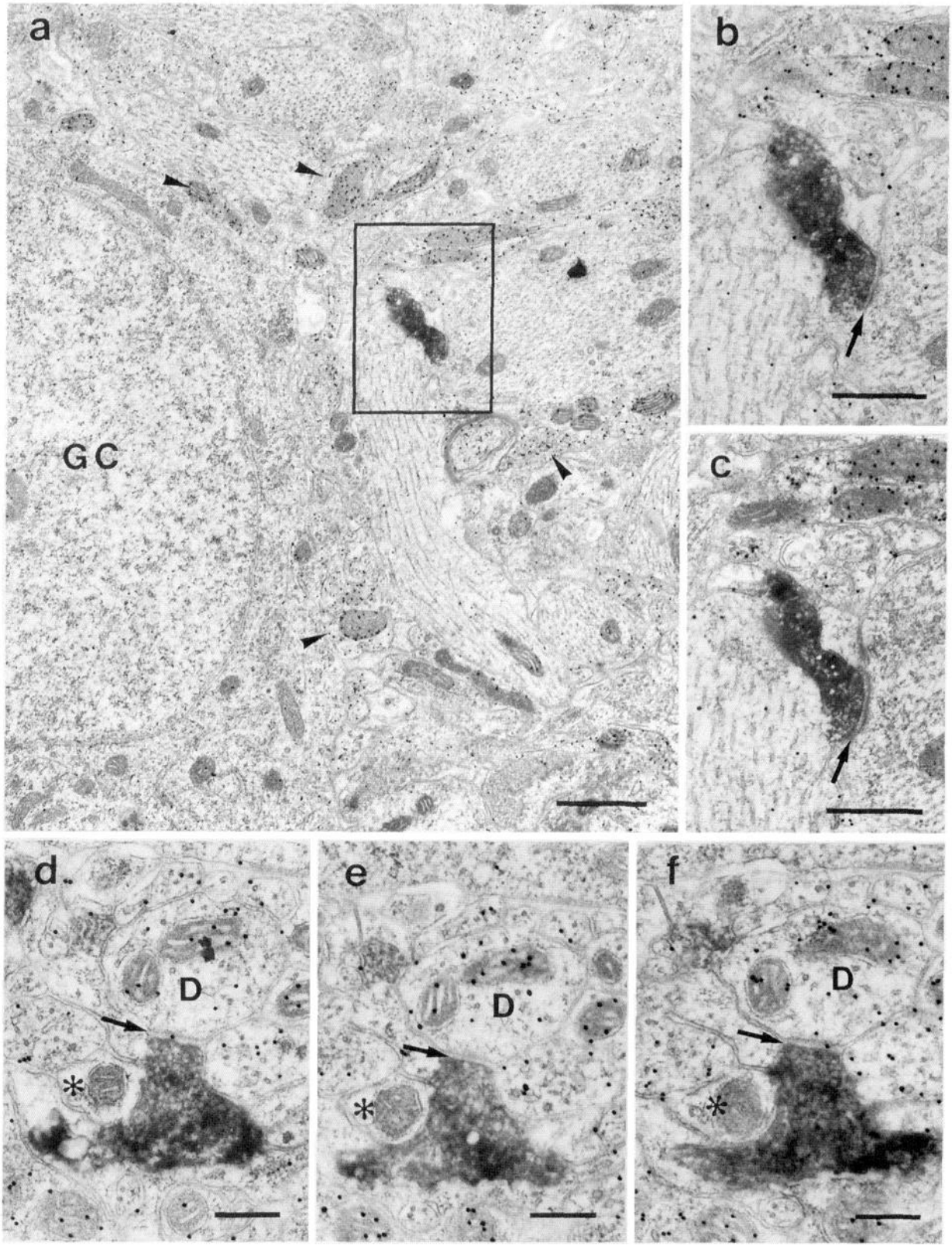

Figure 4. PHAL-labeled entorhinal fibers terminate on GABA-immunopositive and -immunonegative dendrites. *a*, PHAL-labeled entorhinal terminal located within the granule cell layer. Note the specificity of GABA immunostaining; some structures contain large numbers of colloidal gold particles (*arrowheads*), whereas others show only a low background staining. *Framed area* shown at higher magnification in *b* and *c*. *b*, *c*, Serial sections of *framed area* in *a* at higher magnification. Enlargement of the rectangle in *a*. The PHAL-positive terminal forms an asymmetric synapse with a dendritic shaft. Neither the terminal nor the dendrite contains colloidal gold particles. *Arrow* points to synaptic cleft. *d–f*, PHAL-labeled and GABA-negative entorhinal terminal in the IML forming what appears to be an asymmetric synapse with a GABA-positive dendrite (*D*). *Arrow* points to the synaptic cleft. *Asterisk* indicates a GABA-negative profile next to the PHAL-labeled terminal. Scale bars: *a*, 1 μm; *b*, *c*, 0.5 μm; *d–f*, 0.25 μm.

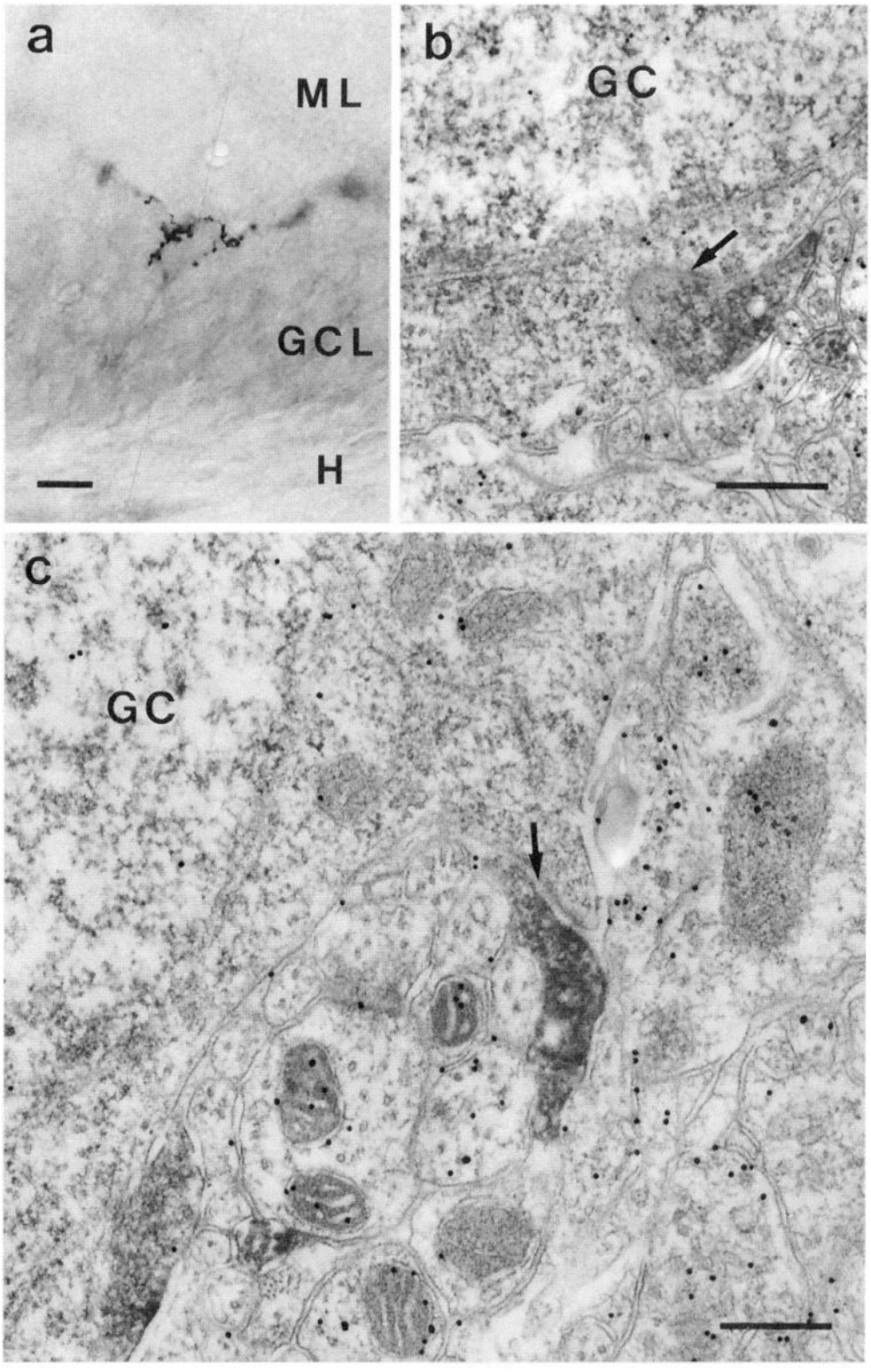

Figure 5. PHAL-labeled entorhinal fibers terminating on granule cell somata. *a*, Photomicrograph of a PHAL-labeled entorhinal axon that forms a basket around a cell in the granule cell layer. *b*, Electron micrograph of a PHAL-labeled entorhinal terminal in the granule cell layer. *Arrow* indicates an asymmetric synapse with a granule cell (*GC*) soma. This section also was processed for GABA postembedding. Note that the PHAL-labeled terminal is GABA-negative. *c*, Electron micrograph of a PHAL-labeled entorhinal terminal in synaptic contact with a somatic spine of a dentate granule cell. This section also was processed for GABA postembedding. The PHAL-labeled terminal is GABA-negative. Scale bars: *a*, 10 μm; *b*, *c*, 0.5 μm.

somatic spines (Fig. 5*c*) of granule cells. Correlated light and electron microscopy of PHAL-labeled entorhinal fibers in the hilus revealed asymmetric synapses on spineless dendrites subjacent to the granule cell layer (Fig. 6*a–d*) and asymmetric synapses on dendrites in the deep hilar area (Fig. 6*e–h*).

The entorhinal projection to the IML, granule cell layer, and hilus does not contain GABA

Postembedding immunocytochemistry for GABA was used to analyze this entorhinal projection for its transmitter content. The postembedding immunocytochemistry was highly specific, and

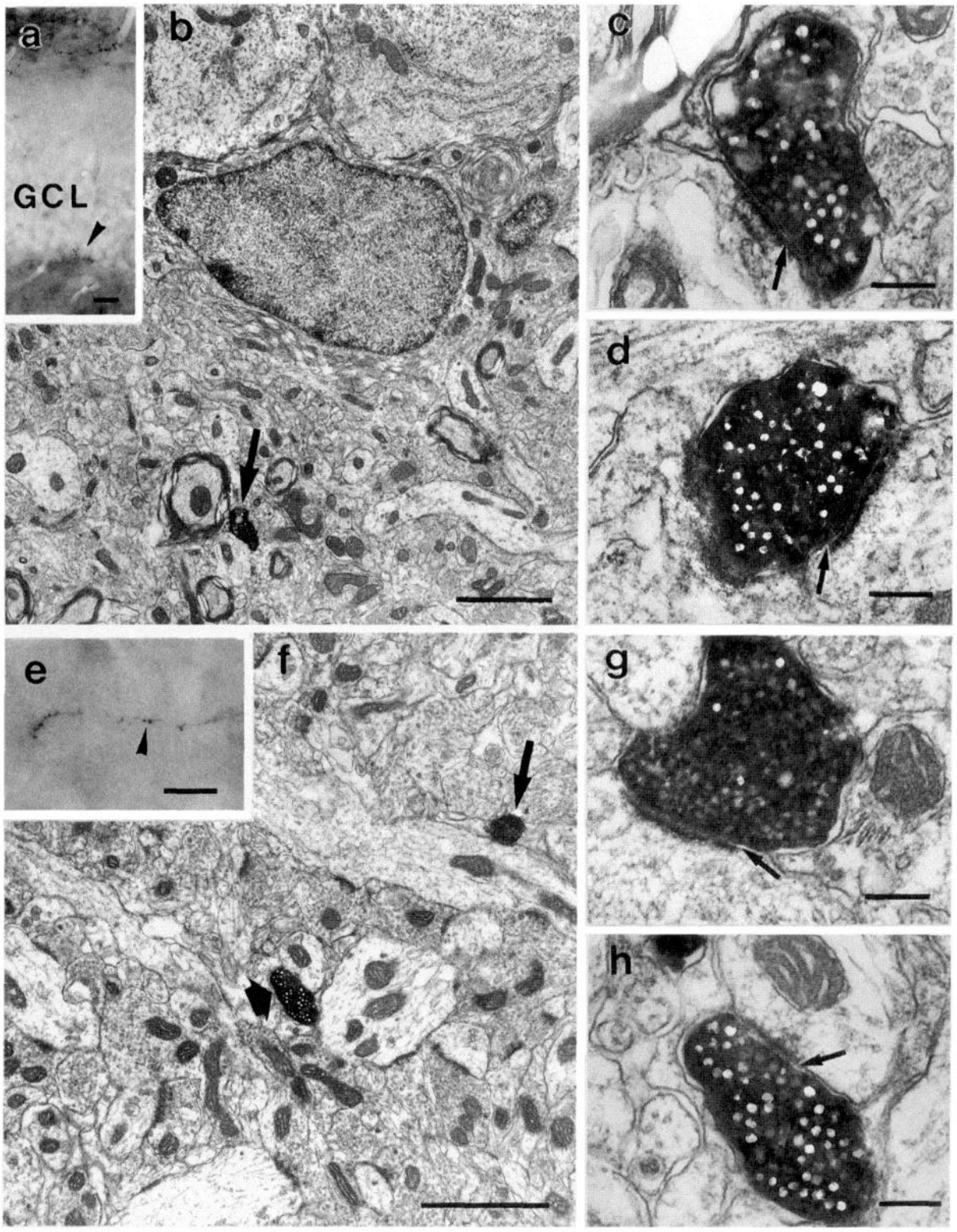

Figure 6. Correlated light and electron micrographs of PHAL-labeled entorhinal fibers subjacent to the granule cell layer and in the hilus. *a*, Low-power magnification to demonstrate side by side the entorhinal projection to the OML and PHAL-labeled boutons subjacent to the granule cell layer (*arrowhead*). *b*, Electron micrograph of the area indicated by *arrowhead* in *a*. A PHAL-labeled terminal is seen subjacent to the granule cell layer. A serial section of this terminal is shown in *c*. *c*, Serial section of the terminal shown in *b*. *Arrow* points to asymmetric membrane specialization. *d*, Electron micrograph of another PHAL-labeled terminal subjacent to the granule cell layer. *Arrow* points to asymmetric contact. *e*, Light micrograph of a section embedded for electron microscopy. *Arrowhead* indicates a PHAL-labeled axon in the hilus of the dentate gyrus. *f*, Electron micrograph of the area indicated by *arrowhead* in *e*. PHAL-labeled entorhinal terminals (*arrows*) are seen in contact with dendritic shafts. Higher magnifications of these terminals are shown in *g* and *h*. *g*, Serial section of the bouton indicated with a *long arrow* in *f*. An asymmetric membrane specialization (*arrow*) with a dendritic shaft is formed. *h*, Higher magnification of the bouton indicated with a *short arrow* in *f*. *Arrow* points to asymmetric membrane specialization. Scale bars: *a*, 20 μm; *b*, 2 μm; *c*, *d*, 0.25 μm; *e*, 10 μm; *f*, 2 μm; *g*, *h*, 0.25 μm.

only very low levels of unspecific background labeling were observed (Fig. 4*a*). Serial sections of PHAL-labeled synapses were examined, and in the investigated material, no PHAL-labeled terminal was found to contain immunolabeling for GABA (Figs. 4, 5*b*,*c*).

The entorhinal projection to the IML, granule cell layer, and hilus is likely to originate from deep entorhinal layers

An attempt was made to correlate PHAL injection sites with the labeling of this entorhinal fiber projection. Figure 1*a* shows the injection site of the animal illustrated in Figure 2. The center of this injection site is located within layers V and VI of the medial entorhinal area. Typically, injections that resulted in the staining of this entorhinal projection were located in the deep layers of the medial entorhinal area and labeled entorhinal fibers to the IML, granule cell layer, and hilus in the infrapyramidal blade (Fig. 2). Injections located exclusively in the deep layers of the lateral entorhinal cortex labeled only very few entorhinal fibers, and these fibers usually were found underneath the suprapyramidal blade. In agreement with earlier reports on the topography of the entorhino-dentate projection (Steward, 1976; Wyss, 1981), injection sites located in the superficial layers of the entorhinal area (layers I–III) only labeled the well known entorhino-dentate projection to the OML.

Topography of the entorhinal projection to the IML, granule cell layer, and hilus

The novel entorhinal projection described here showed a characteristic septo-temporal distribution in serial horizontal sections; in contrast to the entorhino-dentate projection to the OML that leaves the plane of the section, ascends, and terminates in a topographically organized manner along the septo-temporal extent of the hippocampal formation (Steward, 1976; Wyss, 1981) (Fig. 7), the entorhinal fibers to the IML, granule cell layer, and hilus project horizontally to the hippocampus (Fig. 8). This may explain why almost no fibers of this projection are found in septal portions of the dentate gyrus, where entorhinal fibers to the OML are present in large numbers. However, a systematic study with injection sites in various dorso-ventral levels of the entorhinal cortex is required to determine the precise topography.

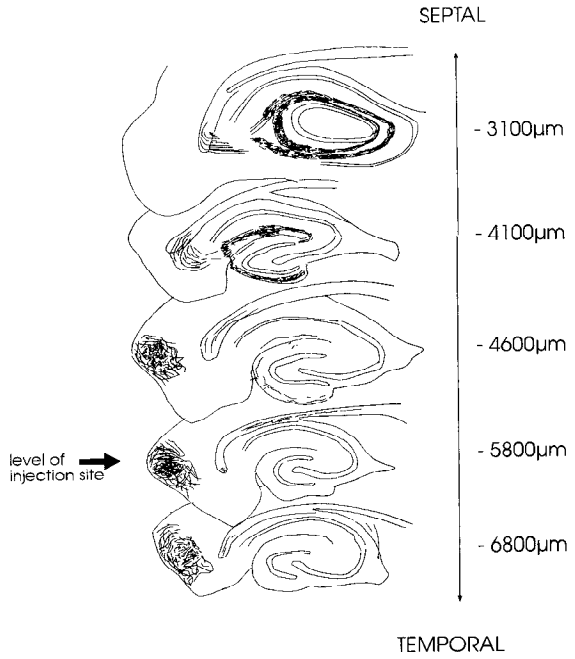

Figure 7. Schematic drawing of the topographical organization of the "classical" entorhino-dentate projection originating from entorhinal cell layers II–III. This drawing illustrates the septo-temporal distribution of entorhino-dentate fibers after a PHAL deposit into layers I–III of the entorhinal area. Camera lucida drawings of five septo-temporal levels are shown (vertical levels given in micrometers from bregma) (Paxinos and Watson, 1986). Almost no fibers can be seen in the dentate gyrus at the level of the PHAL injection site (*arrow*) (septo-temporal extent of the injection site: 500–800 µm). Entorhino-dentate fibers originating in layers I–III follow a rostral trajectory and terminate near the septal pole of the dentate gyrus.

DISCUSSION

In the present study, we have provided evidence for the existence of an entorhinal projection to the IML, granule cell layer, and hilus. This projection originates presumably in the deep layers of the medial entorhinal area and projects horizontally to the temporal part of the hippocampal formation. The axons of this projection are not immunostained for the inhibitory neurotransmitter GABA. They form asymmetric synapses on proximal dendrites in the IML, on the somata of granule cells, and on the spineless shafts of GABAergic dendrites. Our data suggest that this novel entorhinal projection plays an important role in entorhino-hippocampal interaction.

Methodological considerations

The anterograde tracer PHAL used in this study allows the direct visualization of entorhino-hippocampal axons and their terminals and has been shown to be highly sensitive and specific (Gerfen and Sawchenko, 1984). Recently, we have described a previously unknown commissural projection to the OML of the dentate gyrus (Deller et al., 1995) using this technique. It appears to be well suited to analyze the termination and trajectory of small fiber projections that have hitherto escaped detection. Nevertheless, one important objection against the description of a new projection based on the injection of tracer substances is the uptake of tracer by fibers of passage. This appears to be unlikely, because none of the known afferent fiber projections to the molecular layer of the dentate gyrus has a trajectory and termination pattern similar to the one described here for the entorhino-hilar fiber projection traversing the IML. Commissural (Deller et al., 1995), associational (Amaral and Witter, 1989; Deller et al., 1994), and septal axons (Nyakas et al., 1987; Gaykema et al., 1990) enter the hippocampus and fascia dentata via the fimbria and hilus, fibers of hypothalamic origin (Vertes, 1992) terminate directly above the granule cell layer, and the overwhelming majority of noradrenergic and serotonergic fibers terminates within the polymorph layer of the hilus (Conrad et al., 1974; Haring and Davis, 1985). In addition, neither the areas of origin of these projections nor their fiber tracts lie in the vicinity of the present injection sites or the needle tracts, which makes it very unlikely that fibers of these projections could have taken up the tracer.

It is more difficult to rule out the possibility that the entorhino-hilar projection traversing the IML arises from cells of origin located within the subicular complex. This retrohippocampal region is located directly adjacent to the medial entorhinal area and is known to project to the outer two thirds of the molecular layer, as revealed by tracing studies (Caballero-Bleda and Witter, 1993). However, this appears to be unlikely for the following reasons: (1)

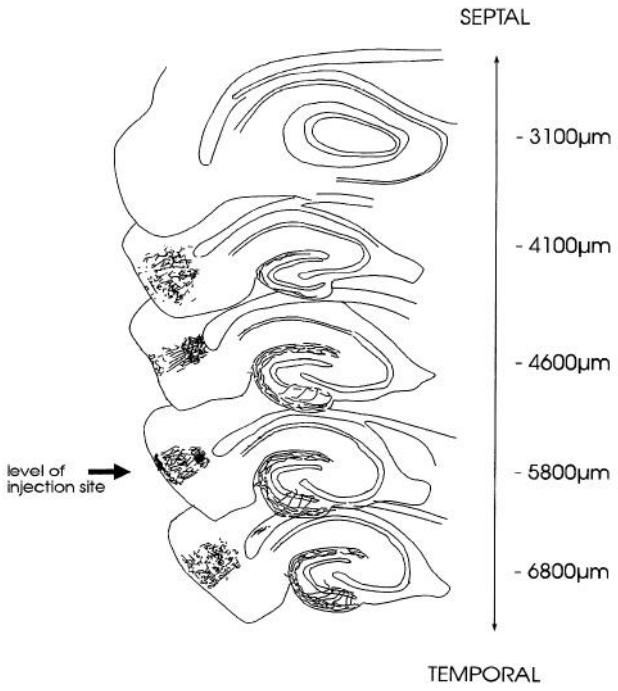

Figure 8. Schematic drawing of the topographical organization of entorhinal fibers to the IML, granule cell layer, and hilus (fibers originating from deep entorhinal cell layers). This drawing illustrates the septo-temporal distribution of entorhinal fibers to the IML after a PHAL deposit into layers IV–VI of the entorhinal area. Camera lucida drawings of five septo-temporal levels are shown (vertical levels given in micrometers from bregma) (Paxinos and Watson, 1986). Entorhinal fibers are found at the same septo-temporal level as the PHAL injection site (*arrow*) (septo-temporal extent of the injection site: 500–800 µm). Near the septal pole of the dentate gyrus, only very few entorhinal fibers are found.

in this study, only animals in which the tracer deposit was located exclusively within the entorhinal cortex were included (Fig. 1); (2) retrograde tracing identified neurons in layers IV and VI of the entorhinal area as entorhino-hippocampal projection neurons (Köhler, 1985a); (3) fibers to the OML of the dentate gyrus arising from the pre- and parasubiculum are arranged radially (Köhler, 1985b; Witter et al., 1988), whereas the fibers described here follow the very characteristic orientation of perforant pathway fibers parallel to the granule cell layer before entering the inner molecular zone; and (4) no PHAL-labeled fibers were observed in the contralateral para- and presubiculum to which the parasubiculum, but not the entorhinal area, projects (Van Groen and Wyss, 1990; Caballero-Bleda and Witter, 1993). Taken together, these observations indicate that the fibers observed in our material do indeed arise from deeper layers of the medial entorhinal area. Because the precise placement of a retrograde tracer into the IML and hilus is technically difficult and will not yield unequivocal results, the identification of the cells of origin of the entorhinal projection to the IML, granule cell layer, and hilus has to await an analysis with sensitive intracellular tracers. Previous studies using horseradish peroxidase as an intracellular tracer (Lingenhöhl and Finch, 1991) did not solve the issue yet.

Lamina-specific termination of fibers in the molecular layer of the dentate gyrus

Entorhinal fibers generally are assumed to be strictly confined to the OML of the dentate gyrus, the so-called "entorhinal" zone. Based on our data, this concept needs to be modified; only fibers that arise from cells located in the superficial layers of the entorhinal cortex are restricted to the outer two thirds of the dentate molecular layer. These fibers project mainly to the septal portion of the hippocampus, where the entorhinal projection to the IML, granule cell layer, and hilus is almost absent. In contrast, fibers that arise from the deeper layers of the entorhinal cortex may leave the classical entorhinal termination zone. These fibers project horizontally to the dentate gyrus. We may conclude that the well known lamination of the dentate gyrus holds true only for the septal pole of the hippocampus, whereas in the temporal pole of the hippocampal formation, entorhinal fibers also terminate in the IML, granule cell layer, and hilus.

Similarly, commissural fibers to the dentate gyrus believed to be restricted to the IML, the so-called "hippocampal" zone (Blackstad, 1956; Zimmer, 1971; Gottlieb and Cowan, 1973; Swanson et al., 1981), recently were demonstrated to give rise to a previously unknown small projection to the OML. This projection differs from that to the IML by its termination pattern and its septo-temporal topography (Deller et al., 1995). Based on these data, the concept of fiber segregation in the dentate gyrus needs to be

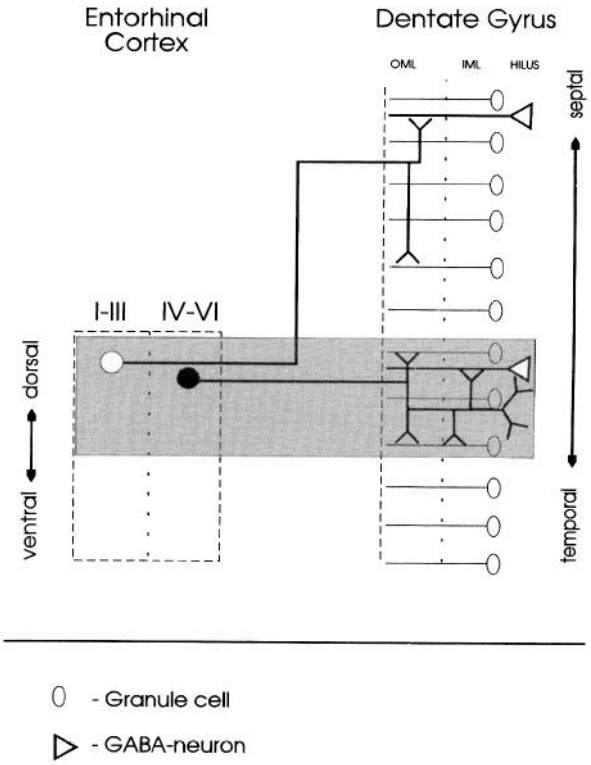

Figure 9. Schematic diagram of entorhino-dentate projections. The diagram shows the entorhinal cortex and the dentate gyrus in their dorso-ventral and septo-temporal (longitudinal) extent. The *gray area* indicates the level of the PHAL deposit. PHAL deposits located in the superficial layers of the dorsal entorhinal area label the "classical" entorhino-dentate projection to the outer two-thirds of the molecular layer. These fibers ascend, turn rostrally, and terminate in the septal portion of the dentate gyrus. PHAL deposits located in deeper layers of the same dorso-medial entorhinal area label entorhinal fibers to the IML, granule cell layer, and hilus in temporal portions of the dentate gyrus. These fibers terminate on proximal dendrites of granule cells, proximal dendrites of GABAergic neurons located with their cell bodies in or directly underneath the granule cell layer, and on hilar dendrites, in addition to their "normal" termination in the OML.

reevaluated, taking into account that different cell populations participate in these projections.

Functional implications

The described novel entorhinal projection may be of functional significance, because it terminates in the area of origin of the commissural–associational projections (Berger et al., 1980; Voneida et al., 1981) including glutamatergic mossy cells (Soriano and Frotscher, 1994) and GABAergic inhibitory neurons. Whereas direct feedforward excitation of granule cells via the perforant path is well established, stimulation of entorhinal fibers also may elicit feedforward inhibition (for review, see Mody and Soltesz, 1994). Morphological data suggest that granule cell inhibition in response to entorhinal stimulation may occur in different ways; at least some entorhino-dentate neurons are GABAergic, indicating a direct inhibition of peripheral granule cell dendrites (Germroth et al., 1989). In addition, asymmetric entorhinal synapses have been demonstrated on peripheral dendrites of GABAergic neurons in the OML (Zipp et al., 1989; Deller and Leranth, 1990; Leranth et al., 1990), indicating feedforward inhibition of granule cells. Here, we suggest a third neuronal circuit that also could lead to feedforward inhibition of granule cells; entorhinal fibers form asymmetric synapses on proximal GABAergic dendrites in the IML and hilus. Because these entorhinal fibers project horizontally, temporal portions of the hippocampal formation, rather than the septal part, would be affected (Fig. 9). Because GABA-negative dendrites in the hilus were similarly contacted by PHAL-labeled entorhino-hilar fibers, our data also would be consistent with an excitatory feedforward loop. It should be pointed out, however, that the majority of fibers originating from the entorhinal cortex terminates in the OML; the functional significance of the entorhinal fibers described here remains to be determined.

The deep layers of the entorhinal cortex differ markedly from the superficial layers in their extrinsic afferent connections. For example, olfactory, perirhinal, septal, amygdaloid, thalamic, prefrontal cortical, temporal cortical, and hippocampal (CA1) fibers terminate in layers I–III, whereas insular, medial prefrontal, and the majority of subicular fibers terminate in layers IV–VI of the entorhinal cortex (for review, see Swanson et al., 1987; Witter, 1993; Amaral and Witter, 1995). The fibers from the deep and superficial layers of the entorhinal cortex in turn differ with respect to their septo-temporal topography; in a given area of the entorhinal cortex, the projection from the superficial layers terminates in more septal portions of the hippocampus (Fig. 7), whereas the projection from the deeper layers innervates more temporal parts (Fig. 8). Taken together, both entorhinal projections appear to differ functionally, affecting different hippocampal lamellae (Fig. 9).

REFERENCES

Amaral DG, Witter MP (1989) The three dimensional organization of the hippocampal formation: a review of anatomical data. Neuroscience 31:571–591.

Amaral DG, Witter MP (1995) The hippocampal formation. In: The rat nervous system, 2nd Ed (Paxinos G, ed), pp 443–494. New York: Academic.

Berger TW, Semple-Rowland S, Basset J (1980) Hippocampal polymorph neurons are the cells of origin for ipsilateral association and commissural afferents to the dentate gyrus. Brain Res 215:329–336.

Blackstad TW (1956) Commissural connections of the hippocampal region in the rat, with special reference to their mode of termination. J Comp Neurol 105:417–537.

Caballero-Bleda M, Witter MP (1993) Regional and laminar organization of projections from the presubiculum and parasubiculum to the entorhinal cortex: an anterograde tracing study in the rat. J Comp Neurol 328:115–129.

Conrad LCA, Leonard CM, Pfaff DW (1974) Connections of the median and dorsal raphe nuclei in the rat: an autoradiographic and degeneration study. J Comp Neurol 156:179–206.

Deller T, Leranth C (1990) Synaptic connections of NPY-immunoreactive neurons in the rat hilar area. J Comp Neurol 300:433–447.

Deller T, Nitsch R, Frotscher M (1994) Associational and commissural afferents of parvalbumin-immunoreactive neurons in the rat hippocampus: a combined immunocytochemical and PHAL study. J Comp Neurol 350:612–622.

Deller T, Nitsch R, Frotscher M (1995) Phaseolus vulgaris-Leucoagglutinin tracing of commissural fibers to the rat dentate gyrus: evidence for a previously unknown commissural projection to the outer molecular layer. J Comp Neurol 352:55–68.

Deller T, Frotscher M, Nitsch R (1996) Sprouting of crossed entorhino-dentate fibers after a unilateral entorhinal lesion: anterograde tracing of fiber reorganization with *Phaseolus vulgaris*-leucoagglutinin (PHAL). J Comp Neurol 365:42–55.

Gaykema RPA, Luiten PGM, Nyakas C, Traber J (1990) Cortical projection patterns of the medial septum-diagonal band complex. J Comp Neurol 293:103–124.

Gerfen CR, Sawchenko PE (1984) An anterograde neuroanatomical tracing method that shows the detailed morphology of neurons, their axons and terminals: immunohistochemical localization of an axonally transported plant lectin, *Phaseolus vulgaris* leucoagglutinin. Brain Res 290:219–238.

Germroth P, Schwerdtfeger WK, Buhl EH (1989) GABAergic neurons in the entorhinal cortex project to the hippocampus. Brain Res 494:187–192.

Gottlieb DI, Cowan WM (1973) Autoradiographic studies of the commissural and ipsilateral association connections of the hippocampus and dentate gyrus of the rat. I. The commissural connections. J Comp Neurol 149:393–422.

Haring JH, Davis JN (1985) Differential distribution of locus coeruleus projections to the hippocampal formation: anatomical and biochemical evidence. Brain Res 325:366–369.

Köhler C (1985a) A projection from the deep layers of the entorhinal area to the hippocampal formation in the rat. Neurosci Lett 56:13–19.

Köhler C (1985b) Intrinsic projections of the retrohippocampal region in the rat brain. I. The subicular complex. J Comp Neurol 236:504–522.

Lee KS, Stanford EJ, Cotman CW, Lynch GS (1977) Ultrastructural evidence for bouton proliferation in the partially deafferented dentate gyrus of the adult rat. Exp Brain Res 29:475–485.

Leranth C, Malcolm AJ, Frotscher M (1990) Afferent and efferent synaptic connections of somatostatin-immunoreactive neurons in the rat fascia dentata. J Comp Neurol 295:111–122.

Lingenhöhl K, Finch DM (1991) Morphological characterization of rat entorhinal neurons in vivo: soma-dendritic structure and axonal domains. Exp Brain Res 84:57–74.

Mody I, Soltesz I (1994) Activity-dependent changes in structure and function of hippocampal neurons. Hippocampus 3:99–112.

Nyakas C, Luiten PGM, Spencer DG, Traber J (1987) Detailed projection patterns of septal and diagonal band efferents to the hippocampus in the rat with emphasis on innervation of CA1 and dentate gyrus. Brain Res Bull 18:533–545.

Paxinos G, Watson C (1986) Atlas of the rat brain in stereotaxic coordinates. New York: Academic.

Somogyi P, Hodgson AJ (1985) Antisera to gamma-aminobutyric acid. III. Demonstration of GABA in Golgi-impregnated neurons and in conventional electron microscopic sections of cat striate cortex. J Histochem Cytochem 33:249–257.

Soriano E, Frotscher M (1994) Mossy cells of the rat fascia dentata are glutamate-immunoreactive. Hippocampus 4:65–70.

Steward O (1976) Topographic organization of the projections from the entrohinal area to the hippocampal formation of the rat. J Comp Neurol 167:285–314.

Swanson LW, Wyss JM, Cowan WM (1978) An autoradiographic study of the organization of intrahippocampal association pathways in the rat. J Comp Neurol 181:681–716.

Swanson LW, Sawchenko PE, Cowan WM (1981) Evidence for collateral projections by neurons in Ammon's horn, the dentate gyrus, and the subiculum—a multiple retrograde labeling study in the rat. J Neurosci 1:548–559.

Swanson LW, Köhler C, Björklund A (1987) The limbic region. I. The septohippocampal system. In: Handbook of chemical neuroanatomy, Vol V, Integrated systems of the CNS, Part I (Björklund A, Hökfeld T, Swanson LW, eds), pp 125–277. New York: Elsevier.

Van Groen T, Wyss JM (1990) The connections of presubiculum and parasubiculum in the rat. Brain Res 518:227–243.

Vertes RP (1992) PHA-L analysis of projections from the supramamillary nucleus in the rat. J Comp Neurol 326:595–622.

Voneida TJ, Vardaris RM, Fish SE, Reiheld CT (1981) The origin of the hippocampal commissure in the rat. Anat Rec 201:91–103.

Witter M (1993) Organization of the entorhinal–hippocampal system. Hippocampus 3:33–44.

Witter MP, Holtrop R, van de Loosdrecht AA (1988) Direct projections from the periallocortical subicular complex to the fascia dentata in the rat: an anatomical tracing study using *Phaseolus vulgaris* leucoagglutinin. Neurosci Res Commun 2:61–68.

Wyss JM (1981) An autoradiographic study of the efferent connections of the entorhinal cortex in the rat. J Comp Neurol 199:495–512.

Zimmer J (1971) Ipsilateral afferents to the commissural zone of the fascia dentata, demonstrated in decommissurated rats by silver impregnation. J Comp Neurol 142:393–416.

Zipp F, Nitsch R, Soriano E, Frotscher M (1989) Entorhinal fibers form synaptic contacts on parvalbumin-immunoreactive neurons in the rat fascia dentata. Brain Res 495:161–166.